Available online at www.sciencedirect.com

SciVerse ScienceDirect

Ceramics International 38 (2012) 2803–2812

CERAMICS INTERNATIONAL

www.elsevier.com/locate/ceramint

Molten salt corrosion of high density graphite and partially stabilized zirconia coated high density graphite in molten LiCl–KCl salt

Jagadeesh Sure, A. Ravi Shankar, S. Ramya, U. Kamachi Mudali *

Corrosion Science and Technology Group, Indira Gandhi Centre for Atomic Research, Kalpakkam 603102, India

Received 2 November 2011; accepted 18 November 2011
Available online 28 November 2011

Abstract

Corrosion studies were performed on uncoated high density graphite and plasma sprayed partially stabilized zirconia (PSZ) coated high density graphite with NiCrAlY bond coat in molten LiCl–KCl eutectic salt at 600 °C for periods of 250 h, 1000 h and 2000 h under inert argon atmosphere. High density graphite showed weight loss while PSZ coated high density graphite showed weight gain. There is no significant attack and degradation of top PSZ coating in molten salt, however microcracks were observed at the bond coat-substrate interface after 2000 h of exposure. PSZ coated high density graphite exhibited excellent corrosion resistance in molten LiCl–KCl salt due to chemical stability and absence of phase transformation as confirmed from scanning electron microscopy, X-ray diffraction and laser Raman studies, however adhesion of the coating has to be improved.

Keywords: C. Corrosion; D. Carbon; D. ZrO_2; E. Nuclear applications

1. Introduction

Pyrochemical reprocessing has been chosen as the best option for reprocessing spent metallic fuels using eutectic mixture of LiCl–KCl molten salt for future fast breeder reactor program in India [1,2]. Graphite is proposed as one of the candidate materials for various equipment in pyrochemical reprocessing plant involving high temperature molten chloride salt environment. Graphite has been considered as a candidate material for crucibles, electrodes and liners in pyrochemical reprocessing [3,4], because of easy fabrication, thermal shock resistance and good high temperature strength [4]. Due to high temperature operation with molten chlorides, pyrochemical processing requires high corrosion resistant materials for the plant application. Various investigations have been carried out on corrosion of structural materials in molten salt focusing on the corrosion under inert atmosphere and in the presence of oxygen and mechanisms involved [5–13]. Due to limited life of application as crucibles and liners, with the requirement of replacement and accumulation of solid waste, the use of graphite for such applications becomes a critical issue. Hence it is important to evaluate the corrosion behaviour of graphite and morphology of attack in the molten salt. Bernardet et al. [14] conducted tests on graphite in molten fluoride salt at 500 °C and showed that graphite undergoes degradation and considerable attack on the surface due to molten salt and it required a protective coating. Moreover pyrolytic graphite [5,15] and oxide ceramic materials like ZrO_2–SiO_2 [5], and yttria stabilized zirconia [10–13] are widely considered as suitable candidate materials for molten salt environment.

It is well known that pure ZrO_2 undergoes phase transformation on heating and cooling. Hence it is required to stabilize the high temperature stable phase usually tetragonal phase [16,17]. Partially stabilized zirconia (PSZ) coatings exhibited excellent thermal stability and maximum thermal cycle life [16]. Zirconia has stability in highly corrosive environments like Cl_2, O_2 and $UO_2Cl_2 + Cl_2$ [15]. Yttria stabilized zirconia coatings on type 316L SS is considered as one of the candidate material for the salt purification vessel and electrorefiner and the coating has shown excellent corrosion resistance in molten LiCl–KCl salt [10,11]. Recently plasma sprayed ZrO_2–Y_2O_3 coating on Inconel713LC alloy tested in molten LiCl–Li_2O salt under Ar–10%O_2 atmosphere also exhibited excellent hot corrosion resistance to molten salt due

* Corresponding author. Tel.: +91 44 27480121; fax: +91 44 27480301.
E-mail address: kamachi@igcar.gov.in (U. Kamachi Mudali).

0272-8842/$36.00
doi:10.1016/j.ceramint.2011.11.051

to dense, continuous and protective top coat [12,13]. Therefore ceramic oxide coatings increase inertness, corrosion resistance and durability of materials in aggressive molten LiCl–KCl salt.

Thermal spray process is a group of process in which plasma spaying is the most common technique for spraying of ceramic oxides as coatings [16,18]. The plasma spray process is an economical method for producing reproducible and durable thick coatings for molten salt applications [9–13]. Oxides are usually coated on graphite substrates by thermal spray process [19–21]. The graphite reactivity and permeability towards oxygen was reduced by thermal spraying of Al_2O_3, ZrO_2 with different bond coats (SiC or Cr_3C_2) [20]. Al_2O_3–13%TiO_2 ceramic coating was vacuum plasma sprayed on graphite substrate to protect from oxidation [21]. Westphal et al. [3] developed a ceramic-lining over graphite crucibles for the separation of salt from uranium during salt distillation process. Cho et al. [22] applied a thermal spray coating of YSZ ceramic on the graphite crucible for cathode processor application. The coating applied was not only to reduce the reaction between uranium and graphite but also to reduce the contact between molten salt containing UCl_3 and graphite [22]. The adhesion between oxides and graphite can be increased with suitable bond coat applied in between them. The aim of this study is to understand the corrosion behaviour and degradation of uncoated high density graphite (HD graphite), and surface protection of HD graphite with PSZ coating as top coat and NiCrAlY as bond coat. Because of excellent stability and corrosion resistance to molten salts [10–13], PSZ was chosen as top ceramic coat over HD graphite.

2. Experimental procedure

2.1. High density (HD) graphite specimens

Commercially available HD graphite used in the present study was procured from M/s Graphite India Limited, India. HD graphite samples of size 10 mm length and 6 mm diameter were prepared for molten salt corrosion test and for coatings by air plasma spray process. The properties of HD graphite specimens are listed in Table 1. The ends of cylindrical HD graphite samples were polished, drilled and threaded for suspending them in molten salt.

2.2. Plasma spray coating

In order to obtain good adhesion between the substrate and coating, the graphite sample surfaces were sand blasted for 10 min. The composition of partially stabilized zirconia (PSZ) powder used for plasma spraying is listed in Table 2. Prior to spraying PSZ coating, a NiCrAlY bond coat of thickness 50 μm was sprayed over HD graphite rods followed by a top ceramic PSZ coating of 300 μm thickness. The coated layers were produced at M/s Plasma Spray Processors, Mumbai by using a METCO 9 MB type plasma gun. The plasma spray process parameters employed for deposition of PSZ are tabulated in Table 3.

Table 1
Properties of high density graphite.

Properties	Value
Maximum particle size (mm)	0.25
Apparent density (g/cm^3)	1.85
Porosity (%)	11–12
Hardness Rockwell	55–70
Electrical resistivity-max. (μohm-cm)	1400–1600
Tensile strength-min. (kg/cm^2)	134

Table 2
Composition of PSZ powder used for plasma spraying.

Material (wt%)	ZrO_2	Y_2O_3	SiO_2	TiO_2	Al_2O_3	Fe_2O_3
PSZ	Balance	7–9	1	0.2	0.2	0.2

Table 3
Parameters used for air plasma spraying of partially stabilized zirconia coating on HD graphite.

Process parameters	Partially stabilized zirconia coating
Plasma spray equipment	METCO 9 MB
Plasma arc current	600 A
Arc voltage	64–70 V
Powder carrier gas	Ar
Secondary gas	H_2
Powder feed rate	2.75 kg/h
Spraying distance	100 mm
Velocity of particles	∼549 m/s

2.3. Molten salt corrosion studies

LiCl and KCl salt weighed and mixed in proper proportions (44.48 wt% LiCl–55.52 wt% KCl) was used to prepare a eutectic composition. All the salt handling operations were done inside the inert argon atmosphere glove box. The chlorinated salt of 400 g was loaded in the corrosion test cell and the cell was loaded in Molten Salt Testing Assembly (MOSTA) under ultra high purity argon atmosphere. The schematic diagram of the molten salt furnace is shown in Fig. 1. The samples were loaded inside the cell by suspending them in the molten salt cell kept in the furnace (Fig. 1) and heated to the desired temperature. When the test temperature was reached the samples were dipped inside the molten salt. In the present study molten salt corrosion test was carried out at 600 °C for 250 h, 1000 h and 2000 h for uncoated and PSZ coated HD graphite samples in ultra high purity (UHP) argon atmosphere.

2.4. Characterization

Uncoated and coated HD graphite samples were cleaned in distilled water and then dried before molten salt corrosion testing. The initial weight and dimensions of the samples were recorded before the corrosion test. After the corrosion test, samples were removed and cleaned in distilled water ultrasonically and dried. Final weight and dimensions of the samples were then measured and the percentage weight

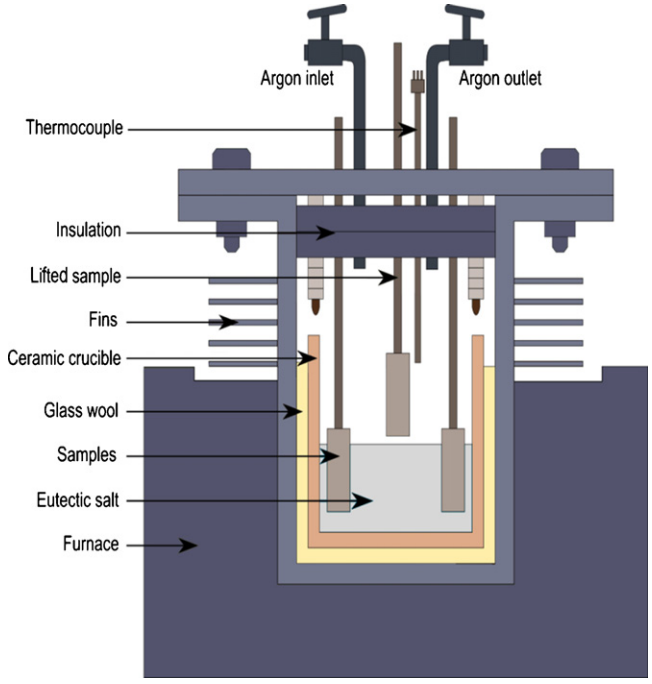

Fig. 1. Molten Salt Test Assembly (MOSTA) setup used for corrosion testing of uncoated and PSZ coated HD graphite.

loss/gain of the samples were calculated. For cross section examination, coated samples were cold mounted with epoxy resin and the mounted samples were prepared according to the ASTM E 1920-03 standard [23]. The as received and corrosion tested uncoated HD graphite samples surface morphology was examined using ESEM (Philips XL-30). The as sprayed and corrosion tested PSZ coated HD graphite samples were examined using scanning electron microscope FEI-Quanta 200F and Carl Zeiss-SUPRA55. The chemical composition of the corroded surfaces was analyzed using energy dispersive X-ray spectroscopy (EDX). XRD studies were carried out with Bruker AXS D8 diffractometer (40 kV, 30 mA, CuK_{α} radiation at 154.056 pm) on as sprayed and corrosion tested PSZ coatings to identify the phase changes and corrosion products formed. The XRD patterns obtained were compared with the standard JCPDF database and available literature.

Raman microscopic experiments were performed on corrosion tested partially stabilized zirconia coated HD graphite specimens using a HR800 (Jobin Yvon) Raman spectrometer equipped with 1800 grooves/mm holographic grating. The samples were placed under an Olympus BXFM-ILHS optical microscope mounted at the entrance of the Raman spectrograph. Argon ion laser of 488 nm was used as an excitation source. The laser spot size of 3 μm diameter was focused tightly on the sample surface using a diffraction limited 10× (NA = 0.25) long distance objective. The laser power at the sample was ≈15 mW. The slit width of the monochromator was 400 μm. The back scattered Raman spectra were recorded using super cooled (<−110 °C) 1024 × 256 pixels charge-coupled device (CCD) detector, over the range 80–2000 cm^{-1} with 5 s exposure time and 20 CCD accumulations. All the spectra were baseline corrected.

3. Results and discussion

3.1. Corrosion studies

The weight change of the HD graphite and its PSZ coated specimens after the corrsion test in molten LiCl–KCl salt for various durations under UHP argon atmosphere was measured. The percentage weight loss of HD graphite for 250 h, 1000 h and 2000 h was 0.033, 0.126 and 0.235, respectively. These results indicate that the weight loss (%) increases linearly with increasing time of exposure. The PSZ coated HD graphite showed insignificant weight gain due to the presence of salt deposits over the surface. It can be inferred from the weight loss measurements that uncoated HD graphite suffers more corrosion attack, when compared to PSZ coated specimens. The weight loss measurements revealed that PSZ coating perform very well in molten LiCl–KCl salt at 600 °C.

3.2. Surface morphology of uncoated HD graphite

SEM micrographs of HD graphite unexposed and exposed to molten LiCl–KCl salt at 600 °C for 250, 1000 and 2000 h are shown in Fig. 2. The increase of molten salt attack with time on HD graphite can be clearly seen from the SEM micrographs of samples exposed to different time periods. The unexposed HD graphite surface contained pores and microcracks as shown in Fig. 2a. The surface morphology of 250 h exposed specimen showed lesser attack and initiation of graphite degradation was clearly seen in the micrograph (Fig. 2b) but the attack was significant in the case of 1000 h exposed (Fig. 2c) and is severe in 2000 h exposed specimens. The mechanism of molten salt corrosion of graphite involves: (1) formation of intercalation compounds, (2) adherence and diffusion of salt into the graphite, and (3) surface porosity filling by molten salt [14]. The molten salt penetrates through pores and interacts with carbon atoms of the graphite surface and dislodges the atoms from its lattice. Hence, it can be inferred from the weight loss measurements and surface morphology results that graphite undergoes substantial attack in molten salt. In the SEM image of 2000 h exposed sample (Fig. 2d) rough surface morphology is observed when compared to unexposed graphite. The graphite particles get dislodged from the surface into the molten salt as the salt particles have penetrated through the surface pores of the HD graphite [14]. Therefore with increase in time of exposure the carbon atoms in graphite start to degrade, which caused material loss, grooves and cavities on the surface as shown in Fig. 2b–d. Throughout the exposed region uniform attack was found on the surface of HD graphite. The pores present in the unexposed graphite surface are more widened after corrosion test. Several oxidants and impurities present in the molten salts are also responsible for accelerating the degradation of HD graphite in LiCl–KCl salt. Comparing the SEM micrographs of HD graphite, it is clear that porosity present in the unexposed graphite increased the weight loss with time of exposure to molten salt. The corrosion behaviour of HD graphite in molten salt suggested that protective coating was essential to avoid degradation in molten salt.

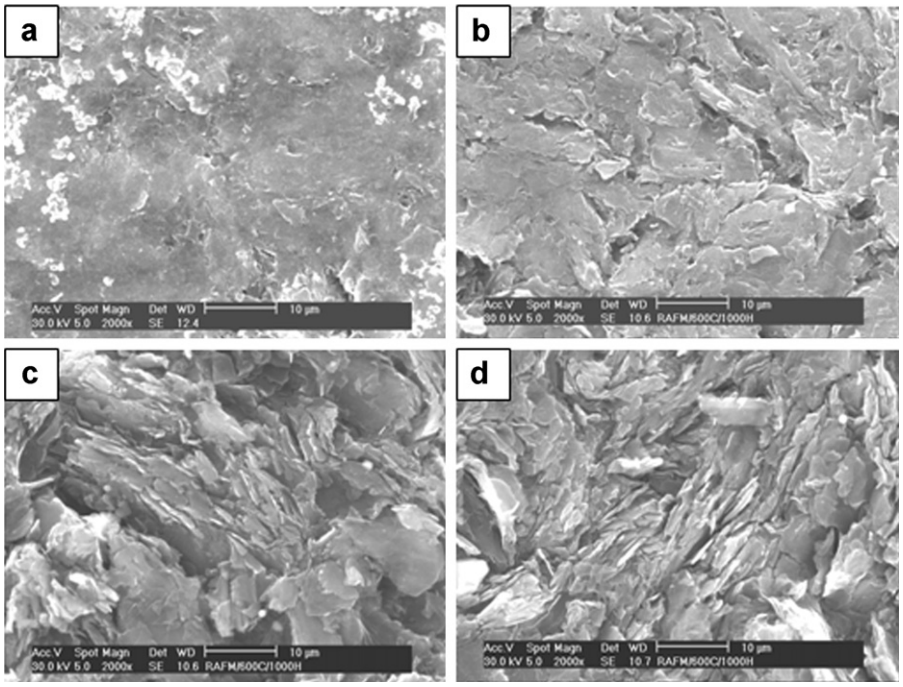

Fig. 2. SEM micrographs of as received and corrosion tested HD graphite in molten LiCl–KCl salt at 600 °C (a) as received, (b) 250 h, (c) 1000 h and (d) 2000 h.

3.3. Surface morphology of PSZ coated HD graphite

The surface morphology of as sprayed coating (Fig. 3a) exhibits typical splat morphology with pores, inter splat voids and microcracks. The presence of impurities like moisture, water and oxygen present in the molten salts will accelerate the corrosion process by dissolution and leaching of the elements [6]. Uniform corrosion, dissolution and leaching are the common form of molten salt corrosion among that selective leaching is very common form at high temperatures [6,8].

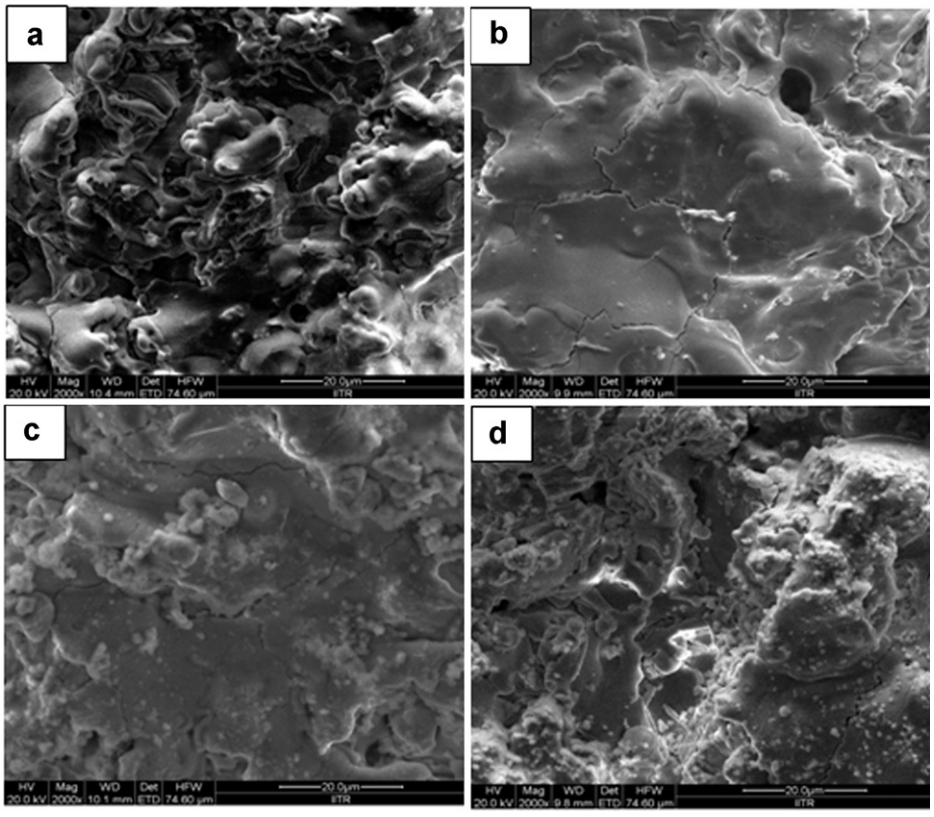

Fig. 3. Surface morphology of (a) as sprayed and immersion tested PSZ coatings in molten LiCl–KCl salt at 600 °C for (b) 250 h, (c) 1000 h and (d) 2000 h.

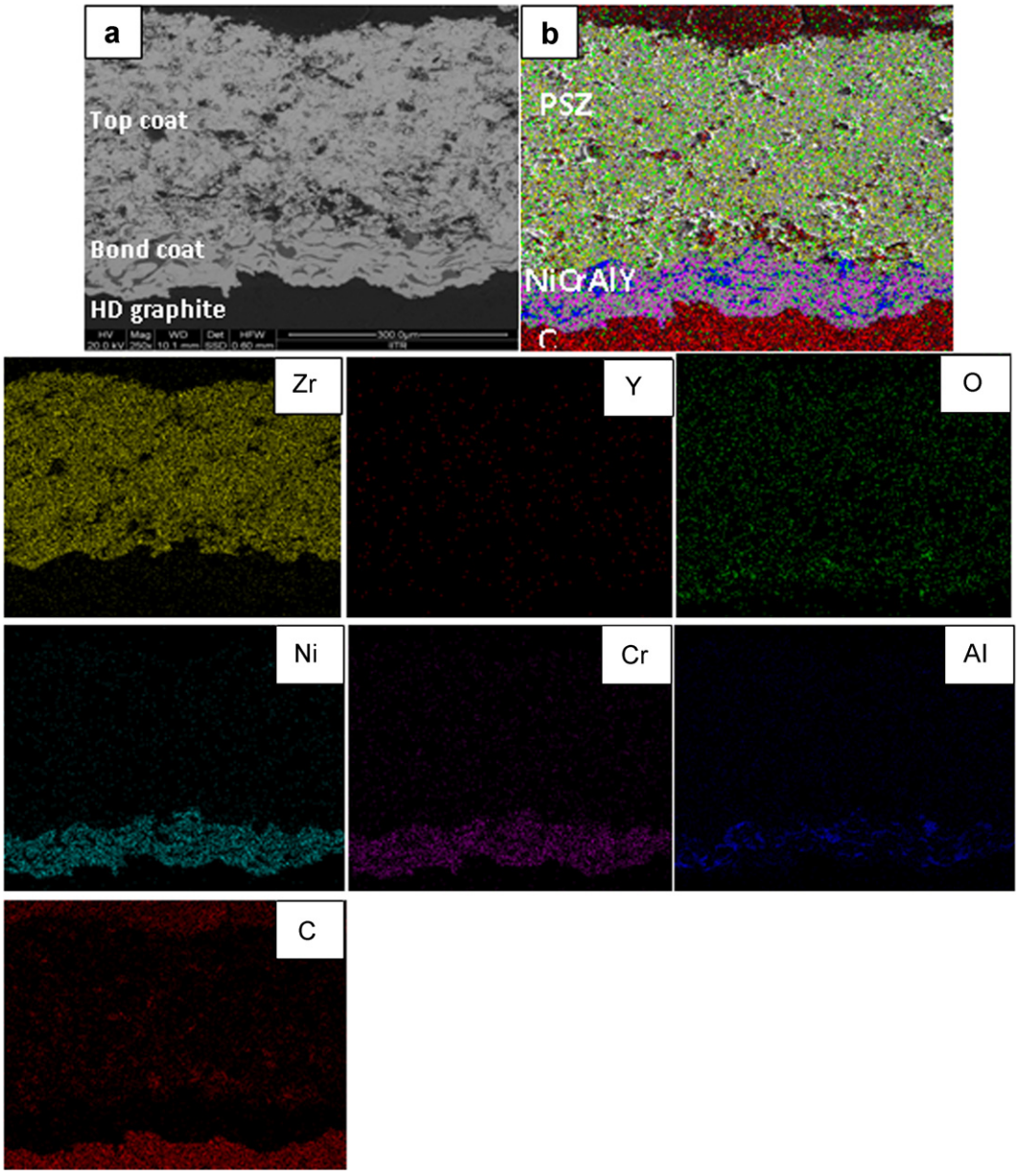

Fig. 4. (a) Cross sectional back scattered SEM images of as sprayed PSZ coating on HD graphite and (b) X-ray elemental mapping of Zr, Y, O, Ni, Cr, Al and C.

Fig. 3b, c and d shows the surface morphology of PSZ coated HD graphite exposed to molten LiCl–KCl salt at 600 °C for 250, 1000 and 2000 h, respectively. Surface morphology of corrosion tested PSZ coating exposed for 2000 h in molten salt was similar to that of as sprayed morphology. All the exposed samples exhibited the formation of dense outer layer and deposition of salt particles over the surface. It was observed that there was insignificant surface chages after corrosion testing in molten salt for 2000 h exposed sample (Fig. 3d). Comparing the surface morphology of corrosion tested YSZ coated on metallic substrate [10,11], it was clear that there was no significant degradation or changes in the surface morphology of YSZ top coat in both cases. The EDX analysis carried out on exposed coatings showed Zr, Y and O elements. The presence of yttrium in the EDX spectrum clearly indicated that no selective leaching and dissolution of yttrium occurred from coating into molten salt. This due to the absence of depletion of Y_2O_3 from PSZ, there was no possibility of destabilization of PSZ in molten LiCl–KCl salt at 600 °C. The possible reaction of ceramics with oxygen and chlorine containing salt was proposed by Haanappel et al. [24] as shown below:

$$MO(s) + Cl_2(g) \rightarrow MCl_2(g) + 1/2O_2(g) \rightarrow MO(s) + Cl_2(g) \quad (\text{where } M = Zr, Y) \tag{1}$$

Oxides have better stability in chlorine environments (Eq. (1)) and the standard Gibb's free enrgy change for the reaction of ZrO_2, Y_2O_3 with chlorine is shown below [15]

$$1/2ZrO_2 + Cl_2(g) \rightarrow ZrCl_4(g) + 1/2O_2(g)\ \Delta G^\circ\ (\text{kJ/mole}) = 79\ (\text{at } 600\,^\circ\text{C}) \tag{2}$$

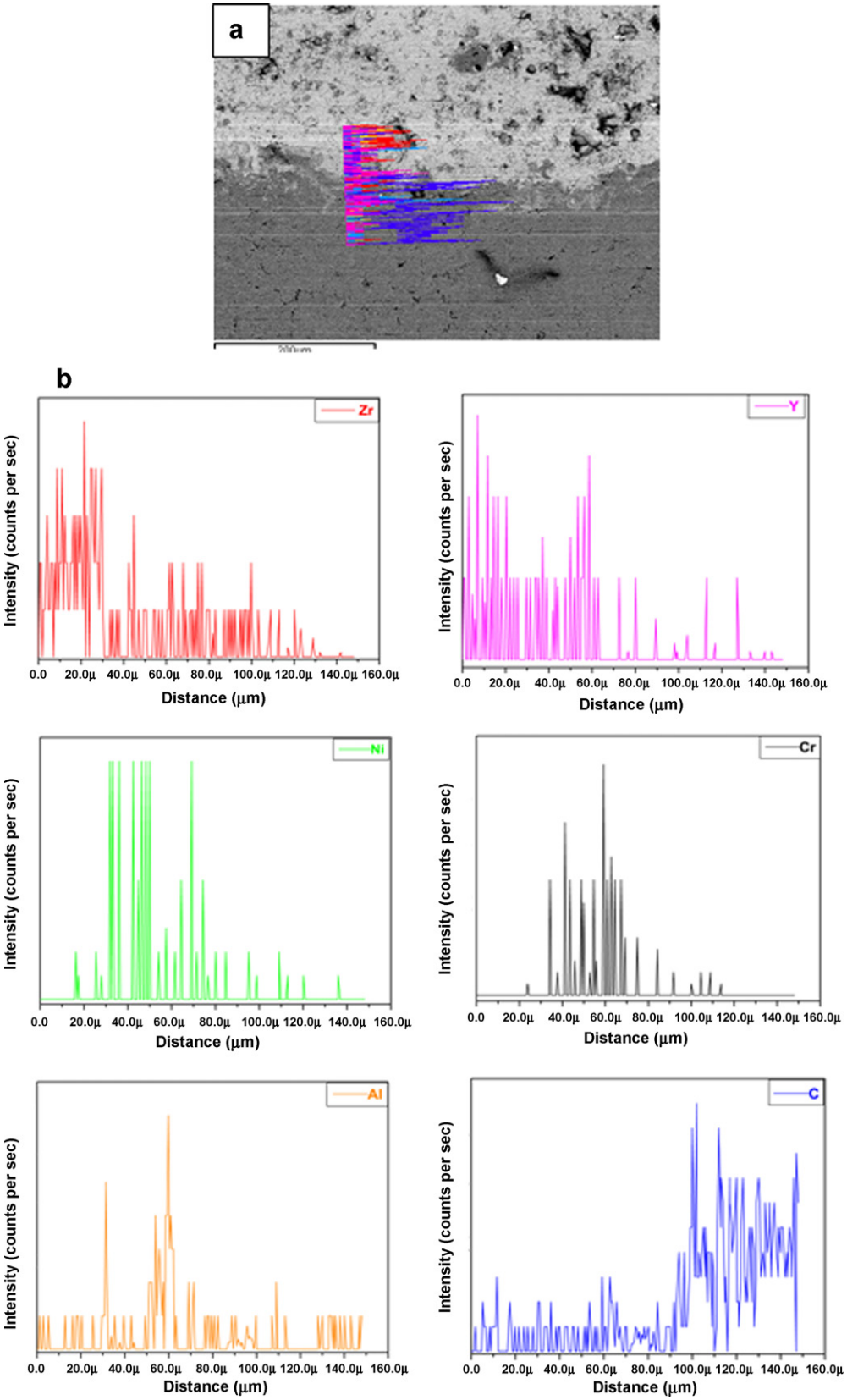

Fig. 5. (a) Cross section of 2000 h exposed PSZ coated HD graphite with NiCrAlY bond coat and (b) corresponding EDX line profiles of Zr, Y, O, Ni, Cr, Al and C elements.

$$1/3Y_2O_3 + Cl_2(g) \rightarrow 2/3YCl_3(g) + 1/2O_2(g)\ \Delta G^{\circ}\ (kJ/mole) = 22\ (at\ 600\ ^{\circ}C) \quad (3)$$

These reactions (Eqs. (2) and (3)) clearly indicated that the yttria stabilized zirconia has good stability. Various defects like pores, voids in between the splats, microcracks and thermal stresses were generated during deposition in the PSZ coatings (Fig. 3a) due to rapid solidification and shrinkage of ceramic particles during plasma spraying. Initially these microcracks and porosity present in the as sprayed coatings act as penetration path for the molten salts. It was repoted that, the dense oxide layer formed on the surface during exposure would prevent further penetration of salt into the coating [12,13]. Thus the attack and dissolution of coating in molten salt has been prevented by the formation of protective dense layer on all the exposed surfaces. The present study revealed that PSZ coating exhibited better corrosion resistance in molten LiCl–KCl salt and provided superior protection to HD graphite.

3.4. Cross sectional studies

Fig. 4a shows the cross section of as sprayed NiCrAlY bond coat followed by PSZ top coat on HD graphite. Top PSZ and bond coats exhibited laminar morphology, which is characteristic microstructural feature of plasma sprayed coatings. The bond coat generally improved the adhesion strength and coating integrity between top ceramic coat and substrate material [12]. X-ray elemental maps of as sprayed coating shown in Fig. 4b clearly indicated that top coat mainly composed of ZrO_2 (Y_2O_3 stabilization) and the bond coat consisted of Ni, Cr, Al and Y. In order to understand the distribution of elements in the exposed coatings, EDX analysis was carried out on cross sections of 1000 and 2000 h samples. The interfaces of PSZ/NiCrAlY and NiCrAlY/graphite were analyzed by EDX line scans on 1000 and 2000 h (Fig. 5a) exposed samples. The elements of Zr, O and Y were distributed in the top coating and, Ni, Cr, Al, Y were present in the bond coat even after the corrosion test for 1000 h and 2000 h test in molten LiCl–KCl salt. The EDX line profiles of 2000 h exposed PSZ coating is shown in Fig. 5b. But a variation in the distribution of elements in 2000 h exposed sample especially in the Ni, Cr and Al line profiles was observed (Fig. 5b). Elements of metallic bond coat particularly Ni, Cr and Al were diffused into HD graphite substrate through pores on the substrate. Cross section SEM micrographs of immersion tested PSZ coated HD graphite after 1000 and 2000 h exposure in molten LiCl–KCl salt are shown in Fig. 6. The top coat of PSZ showed few microcracks in 1000 h (Fig. 6a) and 2000 h (Fig. 6b) exposed samples because of origin of stresses in the coating after exposure to molten salt [25]. Also in case of 2000 h exposed sample the bond coat was discontinuous along cross section and was merged with graphite substrate (Fig. 6b). This could be due to diffusion and formation of chromium carbide, which could lead to spallation. The cross section micrographs does not show any degradation and penetration of salt through the PSZ coating cross section. However microcracks were identified at the interface of NiCrAlY/graphite interface not at the bond coat/

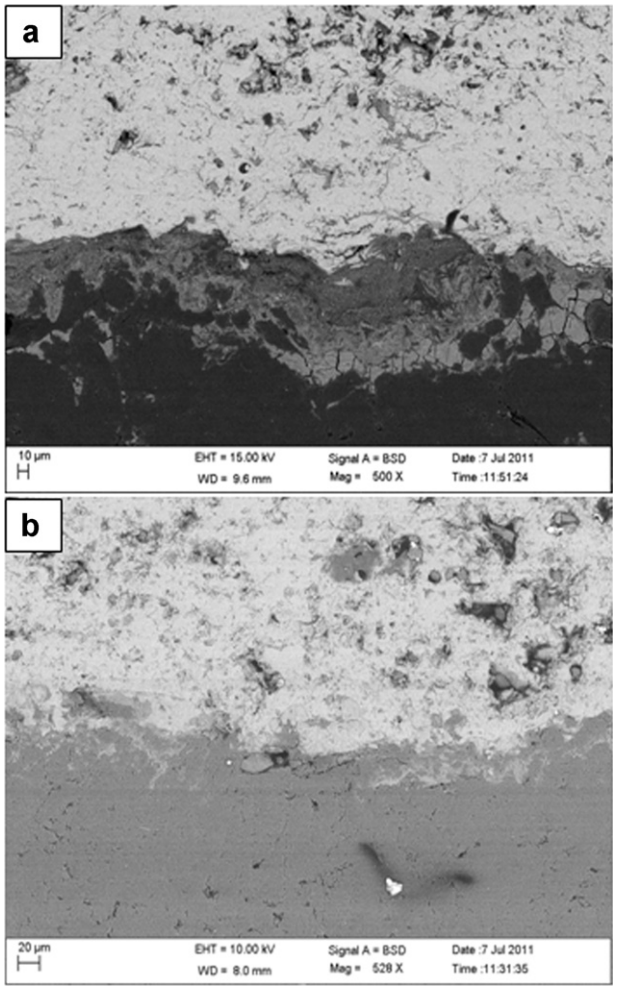

Fig. 6. Cross sections of corrosion tested PSZ coated HD graphite in molten LiCl–KCl salt at 600 °C for (a) 1000 h and (b) 2000 h.

PSZ interface. Formation of cracks in the coating was due to the development of stresses at the bond coat-graphite interface. The mismatch of thermal expansion coefficient between metallic bond coat and HD graphite lead to the development of such stresses at the interface [25]. But no spallation or peel off of coating was observed on HD graphite substrate even after 2000 h test in molten salt.

3.5. XRD studies on PSZ coated HD graphite

XRD pattern of as sprayed PSZ coating on HD graphite is shown in Fig. 7a. According to XRD results as sprayed coatings consisted of tetragonal and cubic phases (Fig. 7a). In plasma sprayed PSZ coatings, zirconia transform to tetragonal modification (t') phase in cubic fluorite matrix [26,27] due to rapid solidification of sprayed powders. This non transformable tetragonal phase has been responsible for excellent strength and crack toughness [16]. After molten salt corrosion, the XRD patterns of the surfaces of 250, 1000 and 2000 h samples are shown in Fig. 7b–d. No new phase corresponding to corrosion product was present in the coating after corrosion test for 2000 h indicating good

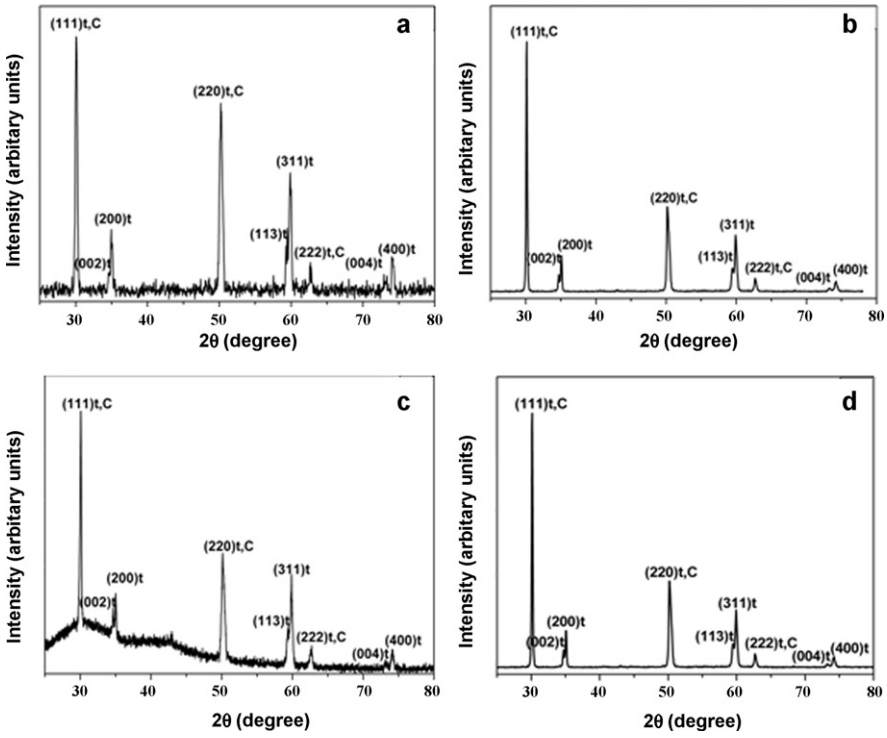

Fig. 7. XRD pattern of (a) as sprayed, (b) 250 h, (c) 1000 h and (d) 2000 h corrosion tested PSZ coated HD graphite in LiCl–KCl salt at 600 °C.

chemical compatibility of PSZ coatings in molten LiCl–KCl salt. Corrosion studies performed in sodium metavanadate molten salts have reported phase transformation from cubic/tetragonal to monoclinic after corrosion test due to leaching of yttrium from the ceramic coating [28]. But there was no phase transformation from tetragonal to monoclinic due to leaching of yttrium was observed from XRD after corrosion test in the present study as shown in Fig. 7a–d. This result was supported by EDX analysis on the exposed PSZ coatings for 250, 1000 and 2000 h. The absence of corrosion products and phase transformations, clearly showed that yttria stablized zirconia on HD graphite was stable in molten LiCl–KCl salt.

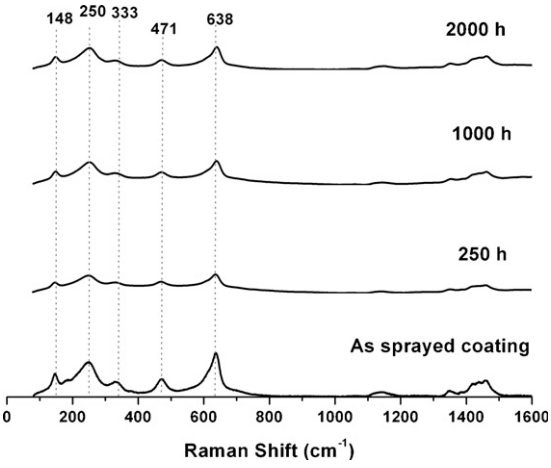

Fig. 8. Raman spectra of as sprayed and corrosion tested PSZ coating over HD graphite for 250, 1000 and 2000 h in LiCl–KCl salt at 600 °C.

3.6. Laser Raman studies on PSZ coated on HD graphite

Raman spectroscopy is an effective tool for the characterization of yttria stabilized zirconia coatings [27–30] to understand the attack of molten salt [28,29]. In the present investigation, Raman experiments were carried out on as sprayed and corrosion tested PSZ coatings in molten LiCl–KCl salt at 600 °C for 250, 1000 and 2000 h to identify the phase changes of yttria stabilized zirconia coatings because of high sensitivity of Raman spectroscopy to these ceramics. The Raman spectra showed (Fig. 8) distinct peaks at 148, 250 and 638 cm^{-1} due to the presence of dominant tetragonal ZrO_2 phase [29,30]. In addition to that, weak peaks were obtained at 333 and 471 cm^{-1} and can be attributed to the tetragonal ZrO_2 phases. However, those peaks were shifted to a large wave number difference due to surface defects and heterogeneities. The major peak positions of all the samples are listed in Table 4. One more observation was that all the Raman spectra were similar in terms of all spectral positions irrespective of the increase in exposure time to molten LiCl–KCl salt. Also, the

Table 4
Raman peak assignments of as sprayed and corrosion tested PSZ coated on HD graphite specimens in molten LiCl–KCl salt for different times of exposure.

Peak position (cm^{-1})	Peak assignment
148	Tetragonal
250	Tetragonal
333	Tetragonal
471	Tetragonal
638	Tetragonal
1142, 1352, 1460	Graphitic carbon impurities
Other small peaks	Un assigned

peaks due to sp^2 carbon impurities were observed in all cases [31]. From Fig. 8, it was clear that Raman spectrum of as sprayed coating was similar to that of corrosion tested samples and the phases present in the as sprayed coating were still observed even after 2000 h at 600 °C. The Raman spectra collected at different regions on corrosion tested PSZ coating revealed same spectral features as observed in Fig. 8. All the spectra contained tetragonal phase along with carbon impurities (Table 4), and no variation or change in spectral positions were observed. This inferred that no phase transformation occurred even after exposure to corrosive molten LiCl–KCl salt environment, and that the top PSZ coatings exhibited excellent corrosion resistance towards molten LiCl–KCl salt. Thus for long term exposure to molten salt, PSZ coating on HD graphite with good bond coat is required to achieve good adhesion to the substrate.

4. Conclusions

Immersion studies performed on HD graphite and PSZ coated HD graphite in molten LiCl–KCl salt at 600 °C under UHP argon for 250, 1000 and 2000 h revealed the following:

1. The weight loss results indicated that HD graphite undergoes degradation in molten salt while PSZ coated HD graphite showed weight gain due to salt deposits present on the exposed surface.
2. SEM micrographs of HD graphite showed that attack was severe with increase in exposure time due to penetration of salt through pores and subsequent removal of carbon particles into molten salt.
3. Surface morphology examination of corrosion tested PSZ coatings for 250, 1000 and 2000 h showed no degradation or attack on the surface of exposed coating to molten LiCl–KCl salt.
4. Cross section examination revealed that microcracks were formed at the interface between bond coat and HD graphite due to difference in thermal expansion coefficient.
5. Yttria stabilized zirconia coating provided superior corrosion resistance to HD graphite because of stable and beneficial non transformable tetragonal zirconia phase present as confirmed by XRD and Raman analysis.
6. The study clearly showed that a suitable bond coat with near thermal expansion coefficient bond coat is required for HD graphite to achieve good adhesion.

Acknowledgements

The authors would like to acknowledge Shri. K. Thyagarajan of CSTG for help in operation of the Molten Salt Test Assembly (MOSTA). The authors would like to acknowledge Prof. Ramesh Chandra of IIT Roorkee and Shri. Shyamala Rao Polaki of IGCAR for FE-SEM.

References

[1] B. Raj, H.S. Kamath, R. Natarajan, P.R. Vasudeva Rao, A perspective on fast reactor fuel cycle in India, Prog. Nucl. Energ. 47 (2005) 369–379.
[2] J.J. Laidler, J.E. Battles, W.E. Miller, J.P. Ackerman, E.L. Carla, Development of pyroprocessing technology, Prog. Nucl. Energ. 31 (1997) 131–140.
[3] B.R. Westphal, K.C. Marsden, J.C. Price, Development of a ceramic-lined crucible for the separation of salt from uranium, Metall. Mater. Trans. A 40 (2009) 2861–2866.
[4] A.R. Brunsvold, P.D. Roach, B.R. Westphal, Design and development of a cathode processor for electrometallurgical treatment of spent nuclear fuel, in: ASME Proceedings of 8th International Conference on Nuclear Engineering, April 2–6, 2000, Baltimore, MD, USA, 2000.
[5] M. Asou, S. Tamura, T. Namba, H. Kamoshida, Y. Shoji, K. Mizuguchi, T. Kobayashi, The corrosion resistance tests of crucible materials for oxide pyro-process, in: Proceedings of International Conference on Future Nuclear Systems (Global'99), Aug 29–September 3, 1999, Jackson Hole, WY, USA, 1999.
[6] T. Tzvetkoff, A. Girginov, M. Bojinov, Corrosion of nickel, iron, cobalt and their alloys in molten salt electrolytes, J. Mater. Sci. 30 (1995) 5561–5575.
[7] A. Ravi Shankar, S. Mathiya, K. Thyagarajan, U. Kamachi Mudali, Corrosion and microstructure correlation in molten LiCl–KCl medium, Metall. Mater. Trans. A 41 (2010) 1815–1825.
[8] J.E. Indacochea, J.L. Smith, K.R. Litko, E.J. Karell, Corrosion performance of ferrous and refractory metals in molten salts under reducing conditions, J. Mater. Res. 14 (1999) 1990–1995.
[9] S.H. Cho, S.B. Park, D.S. Kang, M.S. Jeong, H. Park, J.M. Hur, H.S. Lee, Corrosion behavior of plasma-sprayed Al_2O_3 Cr_2O_3 coatings in hot lithium molten salt, J. Nucl. Mater. 399 (2010) 212–218.
[10] A. Ravi Shankar, U. Kamachi Mudali, R. Sole, H.S. Khatak, B. Raj, Plasma-sprayed yttria-stabilized zirconia coatings on type 316L stainless steel for pyrochemical reprocessing plant, J. Nucl. Mater. 372 (2008) 226–232.
[11] A. Ravi Shankar, U. Kamachi Mudali, Corrosion of type 316L stainless steel in molten LiCl–KCl salt, Mater. Corros. 59 (2008) 878–882.
[12] H.-Y. Lee, K.-H. Baik, Comparison of corrosion resistance between Al_2O_3 and YSZ coatings against high temperature LiCl–Li_2O molten salt, Met. Mater. Int. 15 (2009) 783–787.
[13] S.-H. Cho, B.-H. Park, J.-M. Hur, H.-S. Lee, K.-C. Song, J.-H. Lee, Corrosion behaviour of Y_2O_3–ZrO_2 coatings on IN713LC in a LiCl–Li_2O molten salt, Corros. Sci. 52 (2010) 2353–2364.
[14] V. Bernardet, S. Gomes, S. Delpeux, M. Dubois, K. Guerin, D. Avignant, G. Renaudin, L. Duclaux, Protection of nuclear graphite toward fluoride molten salt by glassy carbon deposit, J. Nucl. Mater. 384 (2009) 292–302.
[15] M. Takeuchi, T. Kato, K. Hanada, T. Koizumi, S. Aose, Corrosion resistance of ceramic materials in pyrochemical reprocessing condition by using molten salt for spent nuclear oxide fuel, J. Phys. Chem. Solids 66 (2005) 521–525.
[16] R.L. Jones, Thermal barrier coatings, in: K.H. Stern (Ed.), Metallurgical and Ceramic Protective Coatings, Chapman and Hall, London, 1996, pp. 194–235.
[17] E. Lugscheider, I. Kvernes, Thermal barrier coatings: powder spray process and coating technology, in: N.B. Dahotre, T.S. Sudarshan (Eds.), Intermetallic and Ceramic Coatings, Marcel Dekker Inc., New York/Basel, 1999, pp. 267–306.
[18] P. Chagnon, P. Fauchais, Thermal spraying of ceramics, Ceram. Int. 10 (1984) 119–131.
[19] N. Mesrati, H. Ajhrourh, N. Du, D. Treheux, Thermal spraying on graphite, in: C. Coddet (Ed.), Thermal Spray: Meeting the Challenges of the 21st Century, Proceedings of the 15th International Thermal Spray Conference, ASM International, OH, (1998), pp. 1501–1512.
[20] N. Mesrati, H. Ajhrourh, N. Du, D. Treheux, Thermal spraying and adhesion of oxides onto graphite, J. Therm. Spray Technol. 9 (2000) 95–99.
[21] D.J. Varacalle Jr., H. Herman, G.A. Bancke, W.L. Riggs II, Vacuum plasma sprayed alumina–titania coatings, Surf. Coat. Technol. 54–55 (1992) 19–24.
[22] C.-H. Cho, Y.-S. Lee, E.-S. Kim, J.-G. Kim, H.-S. Lee, The reactivity with uranium of coating layers by the thermal spraying method, J. Radioanal. Nucl. Chem. 287 (2010) 485–490.

[23] ASTM E 1920-03, 2003, Standard guide for metallographic preparation of thermal sprayed coatings, American Society for Testing and Materials (ASTM) International, West Conshohocken, PA, USA, 2008.
[24] V.A.C. Haanappel, T. Fransen, P.J. Gellings, Chlorine-induced high temperature corrosion: I. Metals and alloys – a review, High Temp. Mater. Processes (New York) 10 (1992) 67–90.
[25] G.R. Heath, P. Heimgartner, G. Irons, R. Miller, S. Gustafsson, An assessment of thermal spray coating technologies for high temperature corrosion protection, Mater. Sci. Forum 251–254 (1997) 809–816.
[26] D.L. Porter, A.H. Heuer, Microstructural development in MgO-partially stabilized zirconia (Mg-PSZ), J. Am. Ceram. Soc. 62 (1979) 298–305.
[27] C.H. Peerry, D.W. Liu, R.P. Ingel, Phase characterization of partially stabilized zirconia by Raman spectroscopy, J. Am. Ceram. Soc. 68 (1985), C-184–C-187.
[28] J.C. Hamilton, A.S. Nagelberg, In situ Raman spectroscopic study of yttria-stabilized zirconia attacked by molten sodium vanadate, J. Am. Ceram. Soc. 67 (1984) 686–690.
[29] M.C. Mayoral, J.M. Andres, M.T. Bona, V. Higuera, F.J. Belzunce, Yttria stabilized zirconia corrosion destabilization followed by Raman mapping, Surf. Coat. Technol. 202 (2008) 5210–5216.
[30] P. Barberis, T. Merle-Mrjean, P. Quintard, On Raman spectroscopy of zirconium oxide films, J. Nucl. Mater. 246 (1997) 232–243.
[31] P.W. May, J.A. Smith, K.N. Rosser, 785 nm Raman spectroscopy of CVD diamond films, Diamond Relat. Mater. 17 (2008) 199–203.